LUND UNIVERSITY

Treatment with p33 Curtails Morbidity and Mortality in a Histone-Induced Murine Shock Model.

Westman, Johannes; Smeds, Emanuel; Johansson, Linda; Mörgelin, Matthias; Olin, Anders; Malmström, Erik; Linder, Adam; Herwald, Heiko

Published in:
Journal of Innate Immunity

DOI:
10.1159/000363348

2014

Link to publication

Citation for published version (APA):
Westman, J., Smeds, E., Johansson, L., Mörgelin, M., Olin, A., Malmström, E., Linder, A., & Herwald, H. (2014). Treatment with p33 Curtails Morbidity and Mortality in a Histone-Induced Murine Shock Model. *Journal of Innate Immunity*, *6*(6), 819-830. https://doi.org/10.1159/000363348

Total number of authors:
8

General rights
Unless other specific re-use rights are stated the following general rights apply:
Copyright and moral rights for the publications made accessible in the public portal are retained by the authors and/or other copyright owners and it is a condition of accessing publications that users recognise and abide by the legal requirements associated with these rights.
• Users may download and print one copy of any publication from the public portal for the purpose of private study or research.
• You may not further distribute the material or use it for any profit-making activity or commercial gain
• You may freely distribute the URL identifying the publication in the public portal

Read more about Creative commons licenses: https://creativecommons.org/licenses/

Take down policy
If you believe that this document breaches copyright please contact us providing details, and we will remove access to the work immediately and investigate your claim.

LUND UNIVERSITY

PO Box 117
221 00 Lund
+46 46-222 00 00

Treatment with p33 (gC1q receptor) Curtails Morbidity and Mortality in a Histone-induced Murine Shock Model

Johannes Westman[1, 2], Emanuel Smeds[1], Linda Johansson[3], Matthias Mörgelin[1], Anders I. Olin[1], Erik Malmström[1], Adam Linder[1], and Heiko Herwald[1]

[1]Department of Clinical Sciences, Division of Infection Medicine, Biomedical Center, Tornavägen 10, SE–22184 Lund, Sweden; [3]Center for Infectious Medicine, Karolinska Institutet, Department of Medicine Huddinge – F59, Karolinska University Hospital, Stockholm, Sweden.

[2]To whom correspondence should be addressed: Department of Clinical Sciences, Lund, Division of Infection Medicine, Lund University, BMC, Floor B14, Tornavägen 10, 221 84 Lund, Sweden, Phone +46-46-2220723, Fax +46-46-157756, e-mail johannes.westman@med.lu.se

Abstract

Collateral damage caused by extracellular histones has an immediate impact on morbidity and mortality in many disease models. A significant increase in the levels of extracellular histones is seen in critically ill trauma and sepsis patients. Here we show that histones are released from necrotic cells in patients with invasive skin infections. Under *in vitro* conditions endogenous p33, an endothelial surface protein also known as gC1q receptor, interacts with histones released from damaged endothelial cells. Further functional analyses revealed that recombinantly expressed p33 completely neutralizes the harmful features of histones, *i.e.* hemolysis of erythrocytes, lysis of endothelial cells, and platelet aggregation. We also noted that mice treated with a sub-lethal dose of histones, develop severe signs of hemolysis, thrombocytopenia and lung tissue damage already 10 min after inoculation. These complications were fully counteracted when p33 was administrated together with the histones. Moreover, application of p33 significantly improved survival in mice receiving an otherwise lethal dose of histones. Together, our data suggest that treatment with p33 is a promising therapeutic approach in severe infectious diseases.

Introduction

During recent years, the role of extracellular histones in systemic inflammatory diseases has attracted a great deal of attention. Histones are normally found in the nucleus where they have an important function in the structural organization of DNA fibers and their packing in the chromosome. Mobilization of histones into the extracellular space is mainly a consequence of cell necrosis, but it can also occur during neutrophil extracellular trap (NET) formation and in some cases upon apoptosis [1,2]. When released from dying or NETotic cells, histones can evoke a number of systemic reactions seen for instance in patients with benign and malign tumors, trauma associated lung injury, systemic lupus erythematosus, or malaria [3-6]. Notably, amongst the highest concentrations of histones are measured in plasma samples from patients with traumatic injury or suffering from severe infectious diseases [3,7,8]. Evidence is accumulating that the release of histones can contribute to considerable complications in these groups of patients. These include for instance the induction of massive inflammatory reactions (cytokine storm), thrombocytopenia, thrombin generation, and host cell necrosis [9-12] and indeed there are many reports showing that the levels of histones in patients correlate well with the severity of the disease [3,4,6,13].

Under pathological conditions histones are known to evoke severe endothelial damage and when intravenously (i.v.) injected at high doses, they can cause death in mice within minutes. In 2009 Xu and colleagues established a lethal LPS murine sepsis model to show that endotoxin challenged mice are rescued when treated with an antibody against histone H4. Moreover, it was found that exogenous applied activated protein C (APC) can cleave histones into non-toxic fragments. Application of heparin has also been described to protect mice by neutralizing extracellular histones [8,9] and similar results were reported when C-reactive protein or thrombomodulin were used [14,15]. Together, these findings suggest that histones are an interesting target for drug development.

The present study was undertaken to identify novel proteins that can counteract the toxic effect of extracellular histones. To this end we here report that p33 (also referred to as globular C1q receptor) binds to and neutralizes all subclasses of histones. In addition we show that p33 dramatically improved survival in mice challenged with an otherwise lethal injection of histones. These data implicate that p33 can be used as treatment in severe infectious diseases.

Materials and methods

Peptides and antibodies

Recombinant histone H1, H2A, H2B, H3.1 and H4 were purchased from Bionordika (Stockholm, Sweden) and bovine calf thymus histones from Roche (Basel, Switzerland). p33 derived peptides and histone derived peptides were synthesized at Biopeptide (San Diego, CA, USA). Polyclonal antisera to p33 were raised in rabbits (Innovagen AB, Lund, Sweden). Peroxidase-conjugated goat anti-rabbit immunoglobulin G was purchased from Bio-Rad Laboratories (Berkeley, CA, USA). Antibodies against Histone H4 (polyclonal chip-grade anti-histone H4) and p33 (mouse monoclonal anti-gC1qr, clone 60.11) were from Abcam (Cambridge, UK).

Bacterial strains

The *E. coli* ATCC 25922 was from the Department of Bacteriology, Lund University Hospital (Lund, Sweden).

Ethics statement

The Institutional Review Board (IRB) at Lund University Hospital approved the study (Protocol #790/2005). Plasma samples and tissue biopsies (Lund University Hospital, Sweden and University of Toronto, Canada) were taken with a written informed consent and the study included patients above 18 years of age. The animal use protocols (#M108-10 and #M327-12) were approved by the local Institutional Animal Care and Use Committee (IACUC), at Malmö/Lund, Sweden. All animals were handled according to the Swedish Animal Welfare Act (SFS 1988:534).

Animals

Female Balb/c mice were from Charles River (Sulzfeld, Germany) and at least 8 weeks old at initiation of experiments.

Blood collection

Peripheral venous blood was collected from healthy human individuals into 2.7 ml 0.109 M buffered sodium citrate tubes (Becton Dickinson). Citrated blood was centrifuged (2000 x g, 10 min, 4°C), the plasma supernatant was aliquoted and stored at -80°C.

Purification of recombinant maltose-binding protein-p33 (MBP-p33)

The pMAL-c2 expression vector (New England Biolabs, Ipswich, MA, USA) and *E. coli* XL1-Blue strain (Stratagene, Heidelberg, Germany) was used to express recombinant MBP-p33. Purification and removal of the MBP-tag was performed as previously described [16].

LPS removal from MBP-p33

Concentrated MBP-p33 was diluted 1:10 in cold 10% (v/v) Triton X-114 (Sigma Aldrich). The protein-detergent mixture was incubated for 30 min at 4°C for Triton X-114 to allow detergent to bind up free LPS. Samples were then incubated for 15 min at 37°C before centrifuging them at 15,000 x g for 15 min. The top aqueous phase containing MBP-p33 was carefully removed into a new tube, and the detergent phase containing LPS was discarded. This procedure was repeated two times. To measure LPS, the ToxinSensor Gel Clot Endotoxin Assay kit (Genscript, Piscataway, NJ, USA) was used according to manufacturer's instruction. The LPS-free MBP-p33 was run through PD-10 (GE Healthcare) columns at least three times to remove residual detergent and concentrated using Amicon Ultra Centrifugal Filter Units 50,000 Nominal Molecular Weight Limit (Millipore, Billerica, MA, USA).

Immunostaining of tissue sections

Snap-frozen tissue collected from the center of infection from a patient with severe cellulitis caused by *S .pyogenes* of M1 serotype was stained. The biopsy was cryostat-sectioned to 8 µm and fixed in ice-cold acetone. Immunofluorescence staining was performed with anti-Histone H4 (Abcam, Cambridge, UK) as previously described [17] and visualized using a Nikon A1R confocal microscope (Nikon Instruments, Amstelveen, the Netherlands). It should be noted that the antibody did not penetrate intact cells and thus no intracellular staining was seen.

Depletion column and in-solution digestion for MS

High abundant plasma proteins were removed with a Human 14 Multiple Affinity Removal Spin Cartridge as described by the manufacturer (Agilent Technologies, Santa Clara, CA, USA). Depleted plasma was concentrated using a Spin concentrator for proteins (5 kDa cut off) according to specific manufacturer's protocols (Agilent Technologies, Santa Clara, CA, USA). Plasma protein mixtures in solution were digested and prepared for MS-analysis as previously described [18].

MS-data acquisition and processing

Biognosys HRM-kit (Biognosys AG, Schlieren, Switzerland) was spiked to each sample according to the manufacturer's instructions. Each sample was analyzed on a Thermo Scientific EASY-nLC II coupled to a QExactive mass spectrometer, using the LC-method as previously described except for a longer gradient, 120-minute. The mass spectrometer was operated using the 'Full MS / AIF' method template. The full precursor mass range of 400 to 1'220 m/z was split into 20 overlapping segments with sizes between 26 m/z and 77 m/z.

Each segment used the following instrument parameter. A precursor scan of the segments mass range was acquired with a resolution of 17'500 and a max ion-trapping time of 1 ms only. Precursor ions within the segments mass range were isolated and fragmented all together by HCD with an AGC target value of 5E5 and a NCE of 25.0 (stepped by 10%). The mass spectra of the fragment ions was acquired with a resolution of 35'000 for a mass range of 200 to 1'800 m/z. Raw files were processed together with the generated assay library using Biognosys Spectronaut software tool [19]. Briefly, Spectronaut applies a decoy scoring approach to calculate a false-discovery rate to each identification [20].

Immunoelectron microscopy

Epon sections of HUVEC cells and lung biopsies infected with the *S. pyogenes* AP1 strain were labeled with gold-conjugated antibodies against histone H4 (10 nm) and p33 (5 nm). Molecular complexes between p33 and histone/gold conjugates (5 nm) were negatively stained with 0.75% uranyl formate. Specimens were subjected to transmission electron microscopy as previously described [21] and examined in a Philips/FEI CM 100 transmission electron microscope at the Core Facility for Integrated Microscopy (CFIM), Panum Institute, University of Copenhagen.

ELISA

Microtiter plates were coated overnight with histones (250 nM) or histone derived peptides (1 μM) in coating buffer (15.9 mM Na_2CO_3, 30 mM $NaHCO_3$, pH 9.6) and stored over night at 4^{o}C. Plates were then washed three times in deionized water, blocked in phosphate buffered saline containing 0.05% Tween-20 (PBST) and 0.5% bovine serum albumin for 30 min at 37^{o}C. After a washing step, plates were probed with MBP-p33 (33 nM) for 1 h at 37^{o}C and binding was detected with a polyclonal antisera against MBP-p33 (1:5000) and a peroxidase-

conjugated antibody against rabbit IgG (1:2500, 1 h, 37°C, Bio-Rad Laboratories). All incubations were followed by a washing step in PBST. When performing a competitive ELISA, microtiter plates were coated overnight with histones (100 nM) and probed with 13 nM MBP-p33 in presence of different p33 derived peptides (50 μM) for 1 h at 37°C. Binding was detected as described above.

Surface Plasmon Resonance

Analyses were performed with a BIAcore 2000 instrument (GE Healthcare, Uppsala, Sweden) using the Sensor Chip CM3 technology at 25°C in a running buffer consisting of phosphate-buffered saline (PBS) without additives. MBP-p33 was diluted into 10 mM sodium acetate, pH 4.0 and 1338 response units were immobilized via amine coupling to each flow cells. One flow cell on each Sensor Chip was subjected to the coupling reaction but without protein, and was used as a control in each experiment for bulk resonance changes. Histones were injected in diluted concentrations (31.25 nM, 62.5 nM, 125 nM, 250 nM, 500 nM) over the coated surfaces (at 45 μl/min in running buffer). Regeneration of MBP-p33 surfaces was obtained by injections of 200 μl of 2 M NaCl and 10 mM glycine at pH 2, and followed by an extensive wash procedure.

Sensorgrams were displayed using the BIA Evaluation 4.1 software (GE Healthcare). After X and Y normalization of data, the blank curves from the control flow cell of each concentration were subtracted, and association (k_a) and dissociation (k_d) rate constants were determined using a Langmuir model for fitting in the evaluation program. The equilibrium dissociation constants (K_D) were calculated from these values.

Viable count assay

An overnight culture of *E. coli* strain ATCC 25922 was grown to mid-log phase in 3% (w/v) Tryptic Soy Broth medium at 37°C on rotation. Bacteria were washed in 10 ml cold 10 mM Tris containing 5 mM glucose, pH 7.5 (Tris-Glucose) and diluted to (2 x 10^6 colony forming (CFU) units/ml) and kept on ice. One volume of bacteria was incubated (1 h, 37°C, rotation) with one volume of histones (500 nM), in presence or absence of 2.5 μM MBP-p33. All samples were diluted and plated on Todd-Hewitt agar plates. The following day, antibacterial activity was determined by counting the number of CFUs on the plates.

***In vitro* hemolysis assay**

Citrated blood (1 ml) was centrifuged (2000 x g, 10 min, 4°C), plasma was removed and replaced by 1 ml PBS. The washing step was repeated two times. Histones were diluted in PBS to 10 μM in presence or absence of 10 μM MBP-p33 to a final volume of 60 μl. Tox-7 lysis buffer and PBS served as positive and negative control, respectively. Three μl washed blood cells (5% v/v) were added to each sample and the samples were incubated (60 min, 37°C on rotation) in a heat block. All samples were centrifuged (2000 x g, 10 min, RT) and the supernatants were transferred to microtiter plates. Absorbance of hemoglobin was measured at 540 nm and histone-induced hemolysis was expressed as percentage of Tox-7 lysis induced hemolysis.

Histone-induced cytotoxicity

The assay was performed with EA.hy926 cells (a permanent human hybrid endothelial cell line) [22] cultured in DMEM containing 10% fetal bovine serum, 100 mM hypoxanthine, 0.4 mM aminopterin, 16 mM thymidine, 100 mg/ml streptomycin and 100 U/ml penicillin. The adherent cells were grown confluent in microtiter plates and washed in 200 μl phenol-free DMEM prior to the experiment. Histones (2 – 4 μM) were diluted in phenol-free DMEM and

pre-incubated with MBP-p33 (10 μM) for 1 h at 37°C. Samples were transferred to the endothelial cells and incubated overnight (16 h, 37°C, 5% CO_2). Supernatants were then transferred onto a new microtiter plates and one volume LDH-substrate mix was added. LDH release was measured at 490 nm using the Tox-7 kit (Sigma Aldrich) according to manufacturer's instructions. Histone-induced LDH release was calculated as percentage of Tox-7 lysis-induced LDH release.

Platelet aggregometry

Platelet aggregation was determined by measuring the optical density of stirred platelet-rich plasma (PRP) over time using an aggregometer (Chrono-Log Corperation, Havertown, PA, USA). Citrated blood from healthy donors was centrifuged at 180 x g for 10 min to obtain PRP. The aggregometer was standardized by placing platelet-poor plasma (PPP) in one channel to represent 100% light transmittance. Platelet aggregation was measured in another channel when calf thymus histones (CTH) (300 μg/ml) were added to PRP in presence of absence of MBP-p33 (0.65 – 6.2 μM). Chart recordings were monitored up to 12 minutes.

Determination of the MBP-p33 concentration in murine plasma samples

Eight mice were injected with MBP-p33 (1.5 mg/animal). After 3 min, 30 min, 2 h and 6 h two mice were euthanized at each time point. Blood was drawn through cardiac puncture and immediately transferred into tubes with 70 μl buffered sodium citrate. Plasma was separated from cells by a centrifugation step (180 x g for 10 min) and stored at -80°C until use. Microtiter plates were coated overnight with a monoclonal antibody against anti-p33 (1:1000, clone 74.5.2, Covance). Plated were then washed in PBS containing 0.05% Tween-20, blocked in blocking buffer (PBST containing 0.5% bovine serum albumin), and probed with

100 µl the murine plasma samples. Binding was detected with polyclonal sera against p33 (1:5000) and a peroxidase-conjugated antibody against rabbit IgG.

In vivo imaging of MBP-p33 in mice

A fluorophore (VivoTag 680XL) was used to label MBP-p33 using the Protein Labeling Kit (PerkinElmer) according to manufacturer's instructions. Mice, anesthetized with isofluorane, were injected with fluorescent MBP-p33 and its distribution was visualized at 3 min, 30 min, 2 h, 6 h and once a day for 7 days using the *In vivo* Imaging System from PerkinElmer (IVIS Spectrum). PBS injected mice served as control. Images were generated using the Living Image v.4.3.1 software (Caliper Lifesciences, Hopkinton, MA, USA).

Histone-induced thrombocytopenia and hemolysis

Mice received an i.v. tail vein injection (200 µl) of 0.75 mg CTH (non-lethal dose) in the absence or presence of 1.5 mg MBP-p33. Sterile PBS was used as control. Mice were euthanized with CO_2 inhalation followed by cervical dislocation. Blood was drawn by cardiac puncture using a syringe filled with 70 µl buffered sodium citrate and then transferred into K2 Microtainer MAP tubes pre-coated with 1 mg EDTA (Becton Dickinson). For platelet analysis, blood cells and platelet counts were determined by a Vetscan HM5 (Abaxis, Union City, CA, USA) according to manufacturer's instructions. For hemolysis assay, blood was centrifuged (180 x g for 10 min) and hemolysis in these plasma samples was measured at 540 nm.

Survival study

Mice received an i.v. tail vein injection (200 µl) of 1.5 mg CTH (lethal dose) in the absence or presence of 1.5 mg MBP-p33. Moribund animals were euthanized and counted as dead at the time point of euthanasia.

Statistical analysis

Statistical analysis was performed using GraphPad Prism, Version 6.00. The P-value was determined by using the unpaired t-test (comparison of 2 groups) or the log-rank test (comparison of survival). All experiments were performed at least three times, if not otherwise mentioned. The bars in the figures indicate standard error of the mean.

Results

Extracellular histones are found in patients with invasive skin infections and septic shock

Elevated levels of circulating nucleosomes have been reported in patients with severe infectious diseases [1,4,6]. However, little is known whether skin infections and subsequent necrosis can serve as a source for extracellular histones. To address this question we employed immunofluorescence microscopy and studied biopsies from a patient with deep tissue destruction (cellulitis) caused by *Streptococcus pyogenes*. As shown in figure 1A, immunostaining with an antibody against extracellular histone H4 revealed large areas without any cell integrity where dissemination of extracellular histone H4 and extracellular DNA was recorded. When biopsies from a healthy donor were analyzed under the same experimental conditions, we found mainly intact intracellular DNA and only minor extracellular levels of the histone (Fig. 1B). Under severe conditions, skin infections can cause systemic reactions and evoke life-threatening complications including sepsis, severe sepsis, and septic shock [23,24]. In order to determine the up-regulation of circulating histone H4 in these patients, we used mass spectrometry (MS) analysis. To this end, levels of histone H4 in plasma were analyzed in patients with septic shock and healthy donors. Figure 1C shows that histone H4 was detectable in all five septic shock patients, while the protein was not found in any of the control samples. Taken together, the analyses of patient samples reveled that histone H4 is found in tissue biopsies and plasma samples from patients with severe infectious diseases.

Necrosis of endothelial cells leads to complex formation of histones and endogenous p33

In the next series of experiments we wished to study the fate of histones released from necrotic cells under *in vitro* conditions. We decided to use human umbilical vein endothelial

cells (HUVECs) and induced necrosis by adding *S. pyogenes* bacteria. Cell necrosis and histone release were then followed by immunodetection with a gold-labeled antibody against histone H4 and subsequent transmission electron microscopy. Figure 1D illustrates that the histone was not released from intact cells, while streptococcal-induced cell damage led to a loss of endothelial cell membrane integrity and the mobilization of histone H4 into the extracellular surrounding (Fig. 1E). We also noted that a significant fraction of the histones was attached to the cell membrane. Recently, we reported that endothelial cells express a negatively charged protein, also known as p33 or globular C1q receptor, which binds to antimicrobial peptides (AMP) and thereby protects cells from a lytic attack [16]. As histones are like AMPs positively charged, we decided to test whether the binding of histone H4 to the endothelial surface is also mediated by p33. Indeed double immunostaining revealed that cell-bound histone H4 binds in close proximity to p33 (Fig. 1E), supporting the notion that p33 can act as histone docking protein. Collectively, these data suggest that histones are released from bacteria-infected necrotic cells and can bind via p33 to the cell surface.

MBP-p33 binds to all subclasses of histones

Our *in vitro* findings prompted us to study the interaction between histones and p33 in more detail. Microtiter plates were therefore coated with five histones (H1, H2A, H2B, H3, and H4) and probed with recombinantly expressed p33 fused to mannose-binding protein (MBP-p33). Figure 2A depicts that MBP-p33 binds to all five subclasses, while MBP alone failed to show an interaction (Suppl. Fig 1). To study this interaction further by negative electron microscopy, we removed the MBP-tag by factor Xa cleavage and purified p33 by gel-filtration. The micrographs depict that p33 (without the MBP-tag) forms a trimer that interacts with all five histones and that one p33 trimer can bind up to three ligands simultaneously (Fig. 2B). Additional surface plasmon resonance experiments were performed to show that all

histones bind with high affinity (lower nanomolar range) to MBP-p33 (Table I). To map the histone-binding site in p33, we synthesized a panel of peptides spanning the entire p33 molecule. These peptides were then used in a competitive ELISA. Figure 3A depicts that TEA20 (net charge +2) is the only peptide that blocks the binding of all five histone to MBP-p33. These results suggest that the aminoterminal part of p33 (positions 115-135) is responsible for the binding to histones. In a similar approach we dissected histone H4 into 6 peptides and performed an indirect ELISA to localize the p33-binding site. As shown in figure 3B, p33 binds exclusively to the most aminoterminal part of histone 4 (peptide MSG20; net charge +7.5), while no binding to the other peptides was detected. To summarize this part, the data reveal that trimeric MBP-p33 can bind up to three histones simultaneously with high affinity. This interaction involves a p33 binding site, located at the amino acid positions 115-135 of p33, and a histone H4 binding site, positioned at the aminoterminal part (amino acid positions 1-20) of the protein.

MBP-p33 blocks the (patho)physiological activities of histones

Having established that MBP-p33 binds with high affinity to histones, we next wished to study whether MBP-p33 can interfere with the (patho)physiological features of histones. As histones have been described to have antimicrobial activity, we first performed viable count assays and tested the effect of histones on *E. coli* strain ATCC 25922. We found that all five histones displayed antimicrobial activity at concentrations between 250 - 500 nM which is in the same range as seen for many AMPs. This effect was almost completely abolished when MBP-p33 was added to the reaction mixture (Figure 4A). In the next series of experiments we tested whether MBP-p33 can block histone-induced hemolysis of human erythrocytes. In the absence of MBP-p33, all five subclasses were very efficient in lysing erythrocytes (especially the arginine-rich histones H3.1 and H4) and also bovine calf thymus

histones (CTH) which is a natural mix of the five histones, showed significant hemolytic activity towards erythrocytes. Figure 4B depicts that pre-incubation of histones with equimolar concentrations of MBP-p33, completely prevented hemolysis and the same findings were noted when p33 without the MBP-tag was used (Suppl. Fig 2). Similar results were obtained in cytotoxicity assays with the endothelial cell line EA.hy926. Here we found that MBP-p33 blocks the release of lactate dehydrogenase (LDH) from histone-treated endothelial cells (Figure 4C). Finally, histones have been described to induce platelet aggregation by forming a complex with human fibrinogen and platelets [9]. We therefore measured histone-induced platelet aggregation over time in the absence or presence of MBP-p33. Our results show that histone-evoked platelet aggregation is dose-dependently counteracted when MBP-p33 was added (Figure 4D). Taken together these results show that all physiological and pathophysiological activities of histones are blocked when they are in complex with MBP-p33.

Half-life and fate of MBP-p33 *in vivo*

Though our *in vitro* data show that MBP-p33 down-regulates the self-destructive features of extracellular histones, systemic histone release has been described to contribute to life-threatening complications [25]. These findings not only suggests that extracellular histones play a crucial role in many inflammatory processes, but they also indicate that the levels of endogenous p33 are not sufficient to completely neutralize their toxic activity. We therefore decided to analyze whether administration of exogenous MBP-p33 in mice can be used as treatment to prevent histone-induced morbidity and mortality. To this end we performed a couple of pilot studies and investigated if i.v. injections of MBP-p33 can evoke deleterious side-effects in mice. Our results show that the application of MBP-p33 (1.5 mg/animal) was well tolerated in the animals and no signs of toxicity or any adverse reactions could be

detected. In the next series of experiments Balb/c mice received an i.v. injection of MBP-p33 (1.5 mg/animal). Blood was collected at different time points by cardiac puncture and plasma MBP-p33 levels were determined by a sandwich ELISA. We noted that the MBP-p33 plasma concentration was less than 80 μg/ml already three minutes after injection and below detection limit after 2 hours (Fig 5A). Considering the molecular weight of trimeric MBP-p33 (226 kDa) the rapid clearance from the plasma was unexpected and we therefore decided to further follow the fate of injected MBP-p33. MBP-p33 was labeled with a fluorescent dye and the i.v. injected protein was detected over time by fluorescence imaging in an IVIS Spectrum station. Figure 5B shows that 3 min after injection strong fluorescence signals were detected especially body parts with less fur (tail, hindlimbs, nose), but also staining in the torso was detected. In contrast to the ELISA data, the intensity of the signals only slowly declined over time and 24 hours after injection similar fluorescence intensities were recorded. The signal was still visible at day 7 (Suppl. Fig 3A). These findings were confirmed when the organs of the injected animals were analyzed. Suppl. Fig. 3B illustrates a strong fluorescence intensity in lung, liver, kidney and spleen after 7 days, suggesting that MBP-p33 has not been cleared from the body and is probably attached to blood vessels and the perfused organs.

p33 prevents histone-induced hemolysis, thrombocytopenia and lung damage *in vivo*

I.v. injections of high histone concentrations into mice can cause 100% mortality within minutes. However, at lower concentrations, histones may disrupt the hemostatic equilibrium and eventually trigger pathological symptoms that resemble many complications also seen under septic shock conditions [8,9,11,26]. To test whether MBP-p33 counteracts these host responses, we injected non-lethal doses of CTH (0.75 mg/animal) i.v. into mice in the absence or presence of MBP-p33. Animals receiving an injection with PBS only were used as control. Ten minutes after injection, mice were euthanized and blood samples collected to prepare

plasma samples. We found that plasma samples from CTH treated animals were hemolytic, while no hemolysis in plasma samples of the CTH and MBP-p33 treated or control mice were detected (Fig. 6A). Thrombocytopenia resulting from platelet depletion can constitute a severe complication in patients with severe infectious diseases. Fuchs and colleagues reported in 2011 that injection of non-lethal doses of histones triggers thrombocytopenia in mice [9] and also in our experiments we measured a significant platelet depletion in blood samples from CTH challenged mice. However, when MBP-p33 was co-administered with CTH, platelet counts were in a similar range as seen in the control samples (Fig. 6B). Because hemolytic disorders often lead to pulmonary damage, we analyzed the lungs of the animals. Scanning electron microscopy revealed that mice injected with CTH suffer from severe pulmonary lesions caused by deposited fibrin fibers and aggregated erythrocytes (Fig. 6C, middle panel). The presence of MBP-p33 clearly decreased these histone-induced effects, though the alveoli still appear to be slightly swollen and some small traces of fibrin and erythrocytes were detected (Fig. 6C, bottom panel). Control lungs from PBS injected mice served as control (Fig. 6C, top panel). All together the *in vivo* data show that co-application of MBP-p33 dramatically diminished morbidity in mice challenged with a toxic dose of histones.

MBP-p33 rescues mice from a lethal dose of histones

In the last set of experiments we wished to test whether MBP-p33 has protective effects against lethal doses of histones. To this end, we performed a survival study with Balb/c mice receiving an i.v. injection of CTH (1.5 mg/animal) in the absence or presence of MBP-p33. Mice were monitored for seven days by measuring body weight and temperature on a daily basis. As reported by others [8,9] we observed that all mice receiving CTH only died within 15 minutes. However, when CTH-challenged mice were treated with MBP-p33, the mortality

rate was as low as 50 % and the first lethal case was recorded two hours after injection (Fig. 7). Note that the surviving mice maintained stable weight and body temperature and fully recovered after a couple of days. When MBP-p33 was injected in the absence of CTH as control, it was found that this treatment did not influence health status, body weight, or temperature. To summarize, here we find that MBP-p33 is a potent inhibitor of histones. Our data also suggest that MBP-p33 is a promising drug candidate for the treatment of histone-mediated complications seen in many pathologic conditions including severe infectious diseases.

Discussion

p33 (also known as globular C1q receptor) was initially described as a receptor for the globular heads of C1q [27]. Later it was found that the protein also interacts with other plasma proteins including vitronectin, high molecular weight kininogen, and the coagulation factors XII and thrombin, respectively [28]. In addition to these ligands, a number of bacterial and viral proteins has been identified that can bind either to surface-bound or intracellular p33 [28]. While the interactions of bacterial proteins with membrane-attached p33 is thought to promote cell adhesion and internalization of the pathogen [29-31], the interaction with viral proteins mainly takes place intracellularly and in some cases this has been shown to suppress virus replication [28]. Recently we reported that p33 exhibits high affinity for another group of proteins/peptides, namely AMPs. Our data show that this interaction impairs the bactericidal and cytotoxic features of AMPs and prevents AMP-evoked cell necrosis [16]. It is noteworthy that extracellular histones and AMPs share common features [32]. For instance, histones are like AMPs highly cationic, either lysine-rich (H1, H2A and H2B) or arginine-rich (H3 and H4) [33]. Moreover, they also exert antimicrobial activity against several Gram positive and negative pathogens and are cytotoxic towards many cell types [8,10,26,33]. These similarities prompted us to study the interaction between p33 and histones in more detail and test whether p33 could be used in therapeutic settings.

Our results show that histones are released from necrotic tissue at the site of infection in patients with streptococcal skin infections and we also recorded elevated histone levels in the plasma samples of patients suffering from septic shock. These findings suggest a chain of events that can provide an explanation for the rise of histones in the circulation of these patients, and this was the starting point for us to study the interaction between p33 and histones in more detail. To this end we performed several biochemical approaches to investigate the histone-p33 interaction by ELISA, surface plasmon resonance, and electron

microscopy. p33 was found to bind all subclasses of histones with high affinity (lower nanomolar range) and further analysis revealed that p33 is able to block all tested functional features of histones; *i.e.* antimicrobial activity, cytotoxic properties, and their ability to evoke platelet aggregation. Our *in vitro* results suggest that cell necrosis and platelet aggregation caused by extracellular histones cannot be completely compensated by endogenous membrane-bound p33. We therefore wished to test whether administration of p33 can be used for therapeutic purposes. For this reason we injected pathological doses of histones i.v. into mice and recorded increased hemolysis, platelet depletion and lung injury. These complications were efficiently prevented when p33 was co-administrated in these experiments. At higher concentrations histones have been shown to evoke death within minutes as reported by Fuchs and colleagues [9]. In their study, the authors were able to demonstrate that killing was triggered by profound thrombocytopenia caused by histone-fibrinogen-platelet complexes [9]. In our experiments we also noted that the injection of lethal histone doses caused 100% mortality in mice (less than 15 minutes). However, when mice were treated with p33, we found that all animals survived the first 2.5 hours and after seven days 50% of all mice not only survived, but also had fully recovered.

These findings may have important therapeutic applications in severe infectious diseases as the early administration of a proper treatment can have a significant impact on the outcome of the disease. Kumar and colleagues for instance reported in 2006 that each hour an antimicrobial therapy is delayed in patients with septic shock, mortality could increase by 7.6% [34]. Many complications seen in these patients are caused by a pathologic overreaction of host defense responses and, thus, it is obvious that targeting the pathogen only cannot dampen these self-destructive reactions because they had already been initiated. As a massive release of histones has an immediate deleterious effect, their inhibition in combination with a conventional antimicrobial treatment is a promising therapeutic approach to overcome this

early critical phase. This in turn can have life-prolonging effects and may facilitate subsequent treatments. Our data show that p33 is a potential drug candidate that can be used in sepsis studies. Taken together, the results presented show that the interaction of p33 with extracellular histones blocks pathologic host responses and that administration of p33 curtails both morbidity and mortality in a murine model for histone-induced shock.

Acknowledgements

We wish to thank Pia Andersson and Maria Baumgarten for excellent technical assistance. This work was supported in part by the foundations of Alfred Österlund, Crafoord, Greta and Johan Kock, Knut and Alice Wallenberg Foundation, Ragnar Söderberg Foundation, Sten K Johnson, Sven-Olof Janson Lifework, the Medical Faculty, Lund University, the Swedish Foundation for Strategic Research, and the Swedish Research Council. There are no conflicts of interest.

References

1. Holdenrieder S, Stieber P, Bodenmuller H, Fertig G, Furst H, et al. (2001) Nucleosomes in serum as a marker for cell death. Clinical Chemistry and Laboratory Medicine 39: 596-605.
2. Saffarzadeh M, Juenemann C, Queisser MA, Lochnit G, Barreto G, et al. (2012) Neutrophil Extracellular Traps Directly Induce Epithelial and Endothelial Cell Death: A Predominant Role of Histones. Plos One 7.
3. Abrams ST, Zhang N, Manson J, Liu TT, Dart C, et al. (2013) Circulating Histones Are Mediators of Trauma-associated Lung Injury. American Journal of Respiratory and Critical Care Medicine 187: 160-169.
4. Amoura Z, Piette JC, Chabre H, Cacoub P, Papo T, et al. (1997) Circulating plasma levels of nucleosomes in patients with systemic lupus erythematosus - Correlation with serum antinucleosome antibody titers and absence of clear association with disease activity. Arthritis and Rheumatism 40: 2217-2225.
5. Gillrie MR, Lee K, Gowda DC, Davis SP, Monestier M, et al. (2012) Plasmodium falciparum Histones Induce Endothelial Proinflammatory Response and Barrier Dysfunction. American Journal of Pathology 180: 1028-1039.
6. Holdenrieder S, Stieber P, Bodenmuller H, Busch M, Fertig G, et al. (2001) Nucleosomes in serum of patients with benign and malignant diseases. (vol 95, pg 114, 2001). International Journal of Cancer 95: 398-398.
7. Kutcher ME, Xu J, Vilardi RF, Ho C, Esmon CT, et al. (2012) Extracellular histone release in response to traumatic injury: Implications for a compensatory role of activated protein C. Journal of Trauma and Acute Care Surgery 73: 1389-1394.
8. Xu J, Zhang XM, Pelayo R, Monestier M, Ammollo CT, et al. (2009) Extracellular histones are major mediators of death in sepsis. Nature Medicine 15: 1318-U1117.
9. Fuchs TA, Bhandari AA, Wagner DD (2011) Histones induce rapid and profound thrombocytopenia in mice. Blood 118: 3708-3714.
10. Kleine TJ, Lewis PN, Lewis SA (1997) Histone-induced damage of a mammalian epithelium: the role of protein and membrane structure. American Journal of Physiology-Cell Physiology 273: C1925-C1936.
11. Xu J, Zhang XM, Monestier M, Esmon NL, Esmon CT (2011) Extracellular Histones Are Mediators of Death through TLR2 and TLR4 in Mouse Fatal Liver Injury. Journal of Immunology 187: 2626-2631.
12. Semeraro F, Ammollo CT, Morrissey JH, Dale GL, Friese P, et al. (2011) Extracellular histones promote thrombin generation through platelet-dependent mechanisms: involvement of platelet TLR2 and TLR4. Blood 118: 1952-1961.
13. Zeerleder S, Zwart B, Wuillemin WA, Aarden LA, Groeneveld ABJ, et al. (2003) Elevated nucleosome levels in systemic inflammation and sepsis. Critical Care Medicine 31: 1947-1951.
14. Abrams ST, Zhang N, Dart C, Wang SS, Thachil J, et al. (2013) Human CRP defends against the toxicity of circulating histones. J Immunol 191: 2495-2502.
15. Nakahara M, Ito T, Kawahara K, Yamamoto M, Nagasato T, et al. (2013) Recombinant Thrombomodulin Protects Mice against Histone-Induced Lethal Thromboembolism. PLoS One 8: e75961.
16. Westman J, Hansen FC, Olin AI, Mörgelin M, Schmidtchen A, et al. (2013) p33 (gC1q Receptor) Prevents Cell Damage by Blocking the Cytolytic Activity of Antimicrobial Peptides. J Immunol.

17. Thulin P, Johansson L, Low DE, Gan BS, Kotb M, et al. (2006) Viable group A streptococci in macrophages during acute soft tissue infection. Plos Medicine 3: 371-379.
18. Karlsson C, Malmstrom L, Aebersold R, Malmstrom J (2012) Proteome-wide selected reaction monitoring assays for the human pathogen Streptococcus pyogenes. Nature Communications 3.
19. Bernhardt OM, Selevsek N, Gillet L, Rinner O, Picotti P, et al. (2012) Spectronaut: A fast and efficient algorithm for MRM-like processing of data
independent acquisition (SWATH-MS) data. Proceedings 60th ASMS Conference on Mass Spectrometry 1–2 (2012).
20. Reiter L, Rinner O, Picotti P, Huttenhain R, Beck M, et al. (2011) mProphet: automated data processing and statistical validation for large-scale SRM experiments. Nature Methods 8: 430-U485.
21. Abdillahi SM, Balvanovic S, Baumgarten M, Mörgelin M (2012) Collagen VI Encodes Antimicrobial Activity: Novel Innate Host Defense Properties of the Extracellular Matrix. Journal of Innate Immunity 4: 371-376.
22. Edgell CJ, Mcdonald CC, Graham JB (1983) Permanent Cell-Line Expressing Human Factor-Viii-Related Antigen Established by Hybridization. Proceedings of the National Academy of Sciences of the United States of America-Biological Sciences 80: 3734-3737.
23. Green RJ, Dafoe DC, Raffin TA (1996) Necrotizing fasciitis. Chest 110: 219-229.
24. Gonzalez BE, Martinez-Aguilar G, Hulten KG, Hammerman WA, Coss-Bu J, et al. (2005) Severe staphylococcal sepsis in adolescents in the era of community-acquired methicillin-resistant Staphylococcus aureus. Pediatrics 115: 642-648.
25. Chaput C, Zychlinsky A (2009) Sepsis: the dark side of histones. Nature Medicine 15: 1245-1246.
26. Kleine TJ, Gladfelter A, Lewis PN, Lewis SA (1995) Histone-Induced Damage of a Mammalian Epithelium - the Conductive Effect. American Journal of Physiology-Cell Physiology 268: C1114-C1125.
27. Ghebrehiwet B, Lim BL, Peerschke EIB, Willis AC, Reid KBM (1994) Isolation, Cdna Cloning, and Overexpression of a 33-Kd Cell-Surface Glycoprotein That Binds to the Globular Heads of C1q. Journal of Experimental Medicine 179: 1809-1821.
28. Ghebrehiwet B, Jesty J, Vinayagasundaram R, Vinayagasundaram U, Ji Y, et al. (2013) Targeting gC1qR Domains for Therapy Against Infection and Inflammation. Adv Exp Med Biol 734: 97-110.
29. Braun L, Ghebrehiwet B, Cossart P (2000) gC1q-R/p32, a C1q-binding protein, is a receptor for the InlB invasion protein of Listeria monocytogenes. Embo Journal 19: 1458-1466.
30. Ghebrehiwet B, Tantral L, Titmus MA, Panessa-Warren BJ, Tortora GT, et al. (2007) The exosporium of B.cereus contains a binding site for gC1qR/p33: Implication in spore attachment and/or entry. Current Topics in Innate Immunity 598: 181-197.
31. Nguyen T, Ghebrehiwet B, Peerschke EIB (2000) Staphylococcus aureus protein A recognizes platelet gC1qR/p33: a novel mechanism for staphylococcal interactions with platelets. Infection and Immunity 68: 2061-2068.
32. Choi KY, Chow LNY, Mookherjee N (2012) Cationic Host Defence Peptides: Multifaceted Role in Immune Modulation and Inflammation. Journal of Innate Immunity 4: 361-370.
33. Hirsch JG (1958) Bactericidal Action of Histone. Journal of Experimental Medicine 108: 925-944.

34. Kumar A, Roberts D, Wood KE, Light B, Parrillo JE, et al. (2006) Duration of hypotension before initiation of effective antimicrobial therapy is the critical determinant of survival in human septic shock. Critical Care Medicine 34: 1589-1596.

Figure legends

Figure 1. **Detection of extracellular histone H4**

Immunostaining of tissue from a patient with cellulitis caused by a *S. pyogenes* infection *(A)* and a healthy volunteer *(B)* are depicted. Histones were detected with an antibody against Histone H4. Histones are stained in green and DNA (DAPI) in blue. Scale bar 25 μm.

(C) Mass spectrometry data on histone H4 release in patients (n=5) with septic shock or healthy donors (n=5). Detectable amounts of histone H4 are presented as extracted ion current, which describes the intensity (area under curve) of a selected precursor mass from all peptides measured.

(D) The endogenous expression of p33 (5 nm gold) on non-infected human umbilical vein endothelial cells (HUVEC) is shown. Note, that almost no release of histone H4 was detected.

(E) Treatment of HUVEC cells with *S. pyogenes* evokes cell necrosis and subsequent release of histone H4 (10 nm gold) that co-localizes with endogenous p33 (5 nm gold). p33 (5 nm gold, arrowheads) and histone H4 (10 nm gold, arrows) were immunostained with gold-labeled antibodies. Scale bar 100 nm.

Figure 2. **MBP-p33 binds to all subclasses of histones**

(A) Microtiter plates were coated with different subclasses of histones (100 nM), probed with maltose-binding protein-p33 (MBP-p33) (8 nM), and detected with a polyclonal antibody against MBP-p33. Data are mean and SE from three separate experiments.

(B) Negatively stained electron micrographs of p33 in complex with gold-labeled histones are shown. The image highlights gold-labeled histones (arrows) that are in complex with p33. Scale bar 15 nm.

Figure 3. **Mapping of binding sites in MBP-p33 and histone H4**

(A) Microtiter plates were coated with histones (250 nM). Plates were then probed with MBP-p33 (33 nM) in the presence of peptides derived from p33 (50 μM). Bound p33 was detected as described in Materials and Methods. The values are the mean from three individual experiments. Peptides that block the binding of p33 to histones are marked with an asterisk (* < 65 % binding).

(B) Microtiter plates were coated with histone H4 derived peptides (1 μM) and probed with MBP-p33 (8 nM). Bound p33 was detected as described in Materials and Methods. Mean and SE from four individual experiments are shown.

Figure 4. **Functional inhibition of histones by MBP-p33.**

(A) p33 neutralizes the bactericidal activity of histones.

Histone H1 (500 nM), histone H2A (500 nM), histone H2B (500 nM), histone H3.1 (500 nM), and histone H4 (250 nM) were incubated with 2 x 10^6 colony forming units (CFU)/ml bacteria (*E. coli* strain ATCC 25922) in the presence or absence of 2.5 μM MBP-p33. Samples were plated on Todd Hewitt agar plates and colonies were counted the following day. Data are mean and SE from three separate experiments. ***, $p < 0.001$, **, $p < 0.01$, *, $p < 0.05$.

(B) MBP-p33 blocks the cytolytic effect of histones.

Histones (10 μM) were incubated with washed human erythrocytes in the presence or absence of 10 μM MBP-p33. Samples were centrifuged and hemolysis was measured at 540 nm in the supernatant. Hemolysis was calculated as percentage of cells treated with Tox-7 Lysis buffer. Data are mean and SE from three separate experiments. ***, $p < 0.001$, **, $p < 0.01$, *, $p < 0.05$.

(C) MBP-p33 inhibits histone-induced lactate dehydrogenase (LDH) release from endothelial cells.

Confluent EA.hy926 cells were treated overnight with histone H1 (4 μM), histone H2A (4 μM), histone H2B (4 μM), histone H3.1 (4 μM), histone H4 (2 μM) or calf thymus histones (CTH) (50 μg/ml) in the presence or absence of 10 μM MBP-p33. LDH release was measured in the supernatant. Cell lysis was calculated as percentage of cells treated with Tox-7 lysis buffer. Data are mean and SE from three separate experiments. ***, $p < 0.001$, **, $p < 0.01$, *, $p < 0.05$.

(D) MBP-p33 prevents histone-triggered platelet aggregation

CTH (300 μg/ml) were added to platelet-rich plasma in the presence or absence of increasing concentrations

of MBP-p33 (0.65-6.2 μM). Platelet aggregation was monitored for 12 minutes. Platelet aggregation was calculated as percentage of light transmission through each sample with platelet-poor plasma in a reference channel. One representative experiment out of three is shown.

Figure 5. **Half-life time of MBP-p33 in murine blood samples and its deposition in the tissue**

(A) MBP-p33 was intravenously (i.v.) injected into Balb/c mice and disappearance of MBP-p33 was measured in the mouse plasma at different time points in a sandwich ELISA.

(B) Fluorescently labeled MBP-p33 was i.v. injected into a Balb/c mouse and its distribution in animals was followed for 24 hours by an IVIS Spectrum station.

Figure 6. ***In vivo*** **effects of MBP-p33 in mice challenged with calf thymus histones**

(A) MBP-p33 prevents histone-induced hemolysis.

Mice were i.v. injected with a non-lethal dose of CTH (0.75 mg/animal) in the presence (n=9) or absence (n=10) of MBP-p33 (1.5 mg/animal) for 2 hours. PBS-treated animals (10 min)

served as control (n=7). Blood was drawn by cardiac puncture and then centrifuged at 2,000 x g. Hemolysis was determined by measuring the absorbance at 540 nm in the supernatants.

(B) MBP-p33 blocks histone-induced thrombocytopenia.

The platelet count was measured in the blood samples from animals treated with CTH, CTH/MBP-p33, or PBS for 2 hours. All platelet counts were determined by a Vetscan HM5.

(C) MBP-p33 prevents histone-induced tissue damage in lungs.

The panel shows representative micrographs of lung section from mice treated with PBS, CTH or CTH/MBP-p33 for 2 hours.

Figure 7. **MBP-p33 rescues mice from a lethal injection of histones**

Mice were subjected to an i.v. injection of a lethal dose of CTH (1.5 mg/animal) in the presence (n=8) of absence (n=6) of MBP-p33 (1.5 mg/animal). Survival was monitored for 7 days.

Table I. Affinity constants for the binding of MBP-p33 to histones

Protein	k_a (M^1sec^1)	k_d (sec^1)	k_D (nM)
Histone H1	5.60×10^4	9.59×10^{-4}	17.1
Histone H2A	9.92×10^4	4.76×10^{-3}	47.9
Histone H2B	2.36×10^5	4.59×10^{-3}	19.4
Histone H3.1	2.48×10^5	6.46×10^{-3}	26.0
Histone H4	5.19×10^5	5.43×10^{-3}	10.5

[1]

[1] Histones were injected at different concentrations over MBP-p33 immobilized on a BIAcore CM3 Sensor Chip (see Materials and Methods).

Figure 1

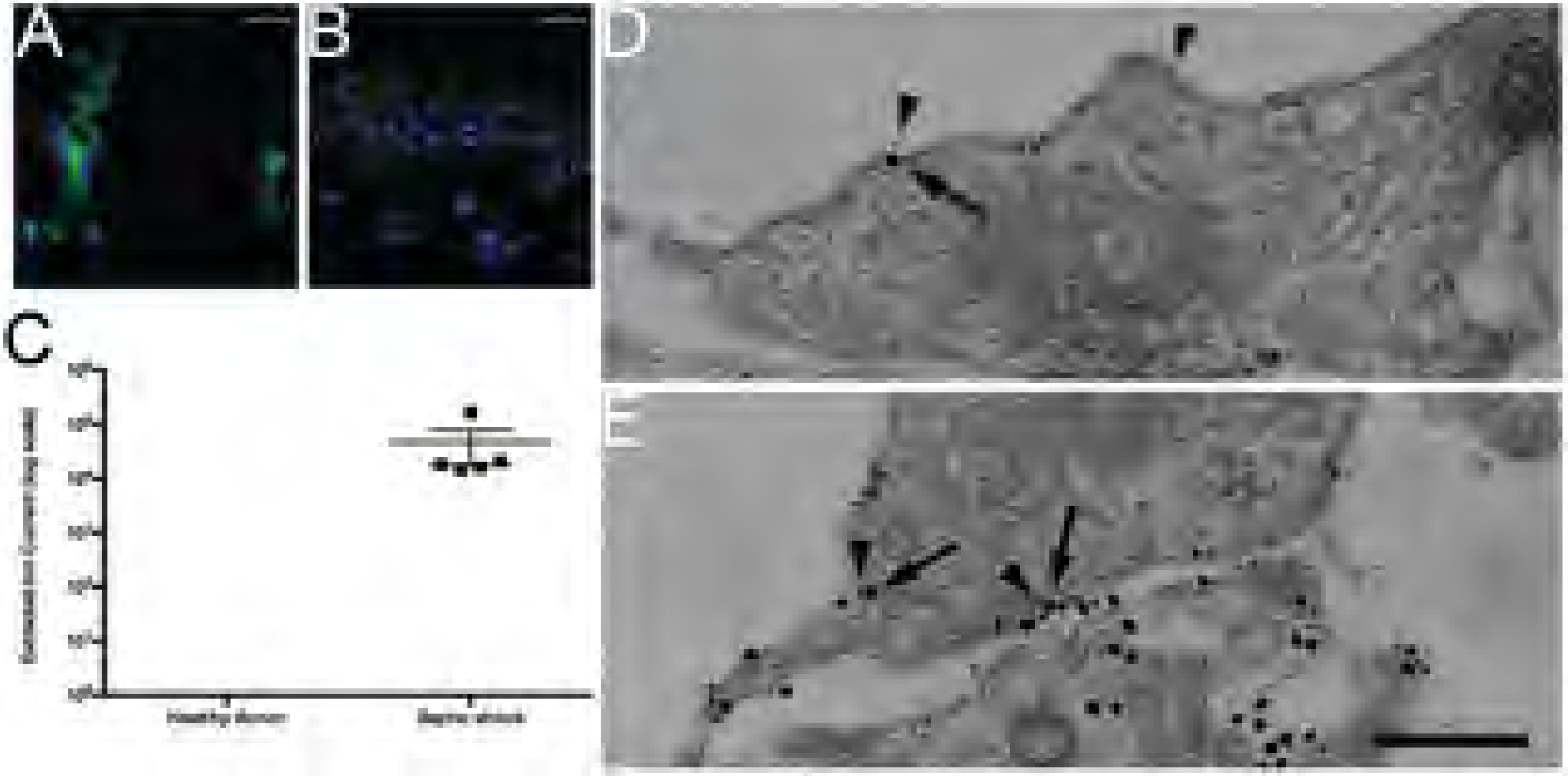

Figure 2

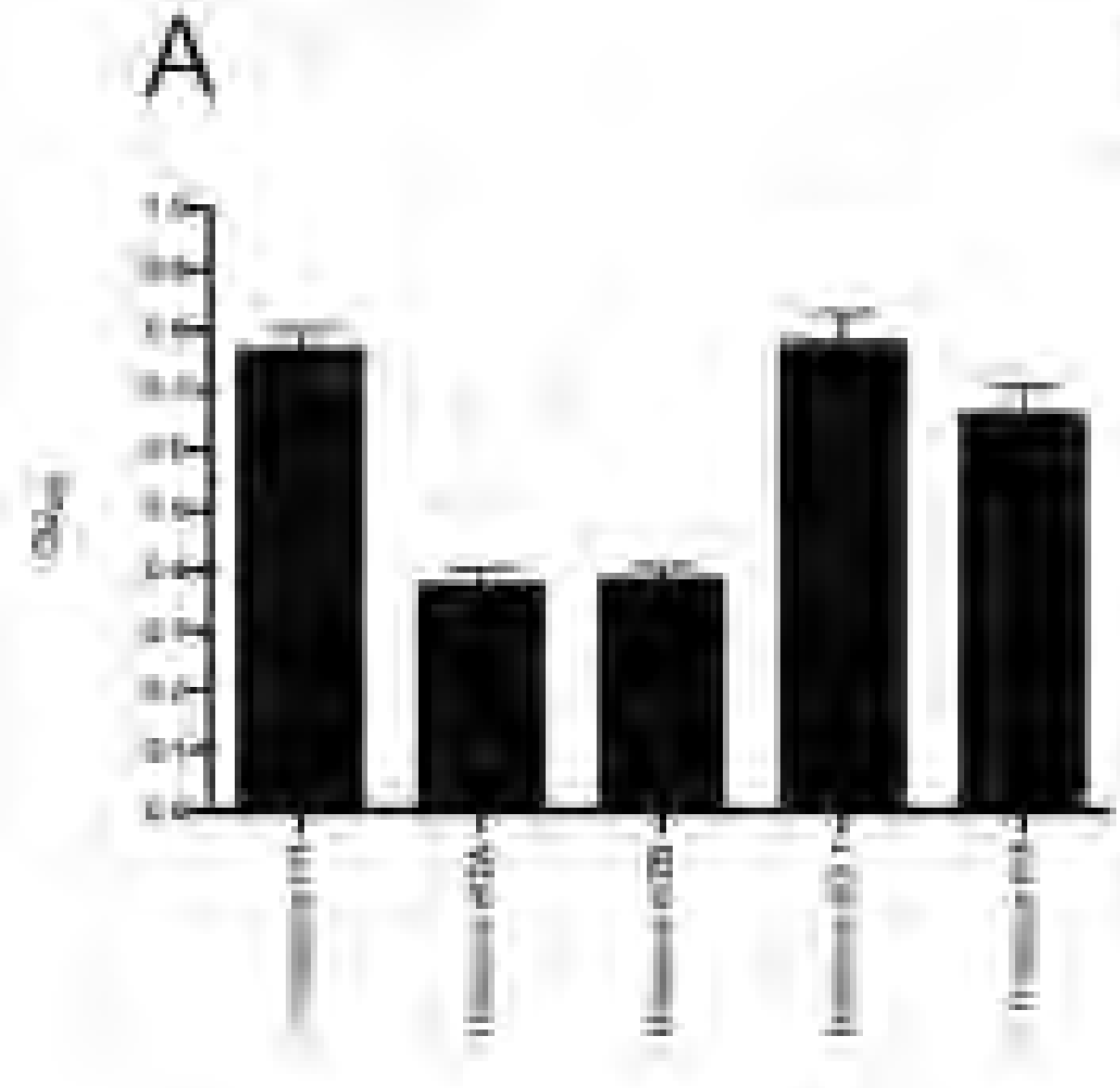

Figure 3

A

p10 peptide		LHT20	DEI20	LPK20	TEA20	TVT20	DGE20	QEP20	VIK20	CHY20	ESD20	TQE20	TDS20	FLA20	LVE20	LEH20
Protein	Charge	+4	+3	-1	+2	-4	-7	-4	-1	-7	-4	-4	-3	-4	-4	-1
Histone H1	+54				+											
Histone H2A	+19				+											
Histone H2B	+19.5				+											
Histone H3.1	+21				+											
Histone H4	+19				+											

B

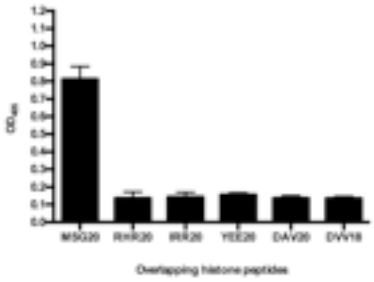

Net charge	+7.5	+6.5	+4	-1	+0.5	+3
Amino acids	1 - 20	18 - 37	35 - 54	52 - 71	69 - 88	87 - 104

Figure 4

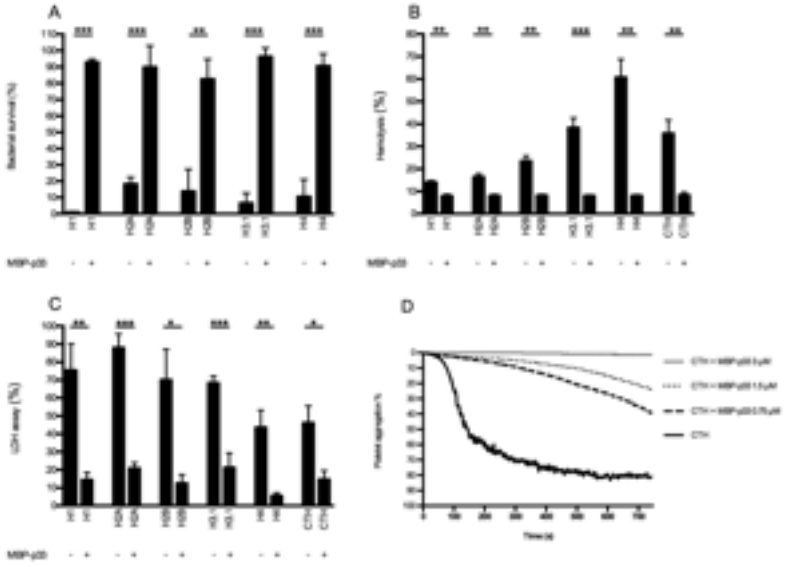

Figure 5

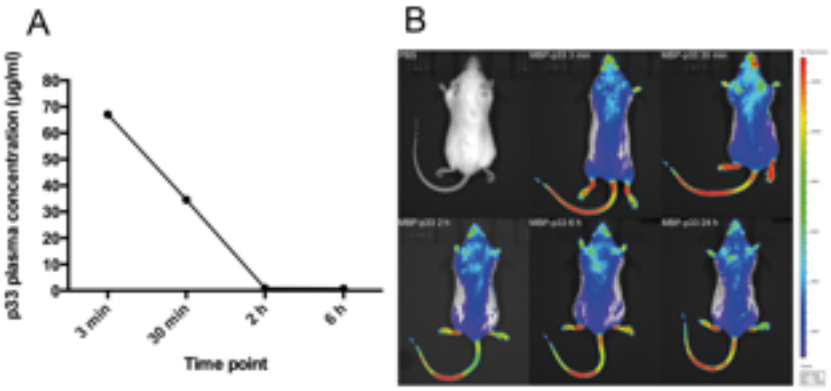
A
B
p33 plasma concentration (µg/ml)
80
70
60
50
40
30
20
10
0
3 min
30 min
2 h
6 h
Time point

Figure 6

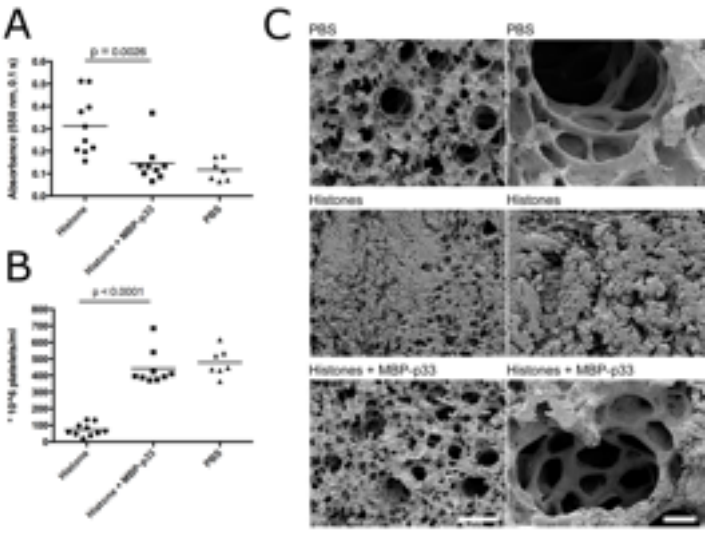
A
p = 0.0026
Absorbance (450 nm, 0.1 s)
Histones
Histones + MBP-p33
PBS
B
p < 0.0001
* 10^6 platelets/ml
Histones
Histones + MBP-p33
PBS
C
PBS
PBS
Histones
Histones
Histones + MBP-p33
Histones + MBP-p33

Figure 7

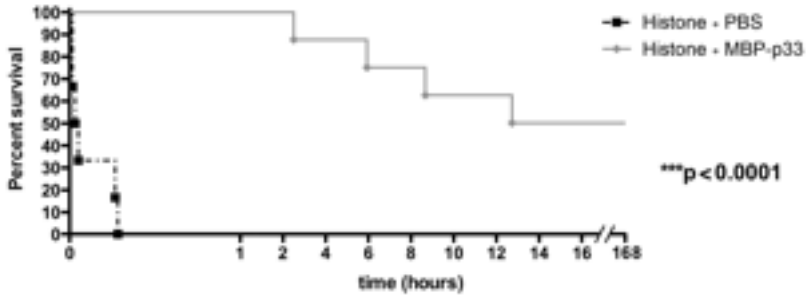
Histone + PBS
Histone + MBP-p33
Percent survival
100
90
80
70
60
50
40
30
20
10
0
0
1
2
4
6
8
10
12
14
16
168
time (hours)
***p < 0.0001

Supplemental data

Supplemental Materials and Methods

ELISA

Microtiter plates were coated overnight with histones (100 nM) in coating buffer (15.9 mM Na_2CO_3, 30 mM $NaHCO_3$, pH 9.6) and stored over night at 4°C. Plates were then washed three times in deionized water, blocked in phosphate buffered saline containing 0.05% Tween-20 (PBST) and 0.5% bovine serum albumin for 30 min at 37°C. After a washing step, plates were probed with MBP (8 nM) for 1 h at 37°C and binding was detected with a polyclonal antisera against MBP-p33 (1:5000) and a peroxidase-conjugated antibody against rabbit IgG (1:2500, 1 h, 37°C, Bio-Rad Laboratories). All incubations were followed by a washing step in PBST. The polyclonal antisera against MBP-p33 was tested to detect MBP and MBP-p33 equally in equimolar concentrations.

In vitro hemolysis assay

Citrated blood (1 ml) was centrifuged (2000 x g, 10 min, 4°C), plasma was removed and replaced by 1 ml PBS. The washing step was repeated two times. Histone H4 were diluted in PBS to 10 μM in presence or absence of 10 μM native p33 to a final volume of 60 μl. Tox-7 lysis buffer and PBS served as positive and negative control, respectively. Three μl washed blood cells (5% v/v) were added to each sample and the samples were incubated (60 min, 37°C on rotation) in a heat block. All samples were centrifuged (2000 x g, 10 min, RT) and the supernatants were transferred to microtiter plates. Absorbance of hemoglobin was measured at 540 nm and histone-induced hemolysis was expressed as percentage of Tox-7 lysis induced hemolysis.

In vivo imaging of MBP-p33 in mice

MBP-p33 was labeled with a fluorochrome (VivoTag 680XL) using Protein Labeling Kit (PerkinElmer) according to manufacturer's instructions. Mice, anesthetized with isofluorane, were injected i.v. with fluorescent MBP-p33 and its distribution was visualized every day for 7 days using the *In Vivo* Imaging System from PerkinElmer (IVIS Spectrum). At time points 1 h and 1 day, mice were sacrificed and MBP-p33 distribution in different organs was visualized. PBS injected mice served as control.

Supplemental Figure legends

Supplemental Figure 1. **MBP does not bind to histones**

Microtiter plates were coated with different subclasses of histones (100 nM), probed with MBP (8 nM) and detected with a polyclonal antibody against MBP-p33. Mean and SE from three individual experiments are shown.

Supplemental Figure 2. **Native p33 inhibits the cytolytic activity of histone H4 against erythrocytes.** Histone H4 (10 μM) were incubated (60 min at 37^{o}C) with washed and diluted human erythrocytes (5% v/v) in the absence or presence of 10 μM p33. Samples were centrifuged and the release of hemoglobin was measured in the supernatant at 540 nm. Hemolysis was calculated as percentage of cells treated with Tox-7 Lysis buffer. Data are mean and SE values from three separate experiments.

Supplemental Figure 3. **Deposition of injected MBP-p33 in mice.**

(A) Fluorescently labeled MBP-p33 was i.v. injected into a Balb/c mouse and its distribution and deposition in animals was followed for 7 days by an *IVIS* Spectrum station. PBS was used as a control.

(B) Organs from mice injected with fluorescently labeled MBP-p33 at time points day 1 and day 7. PBS was used as a control.

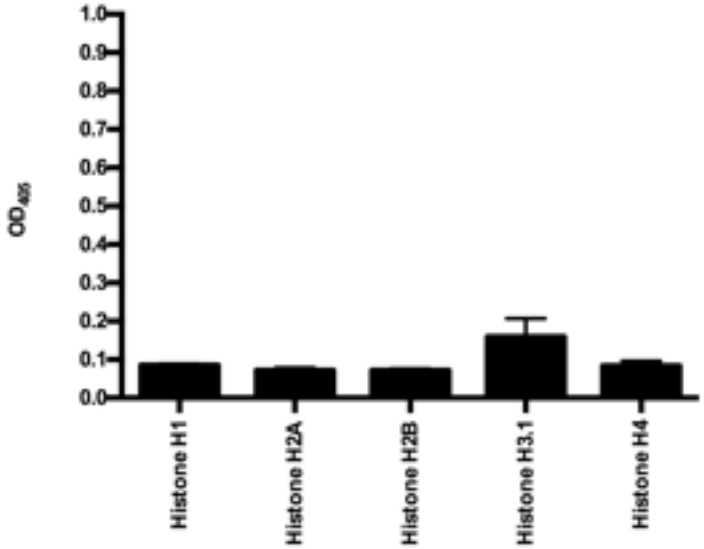
1.0
0.9
0.8
0.7
0.6
0.5
0.4
0.3
0.2
0.1
0.0
OD405
Histone H1
Histone H2A
Histone H2B
Histone H3.1
Histone H4

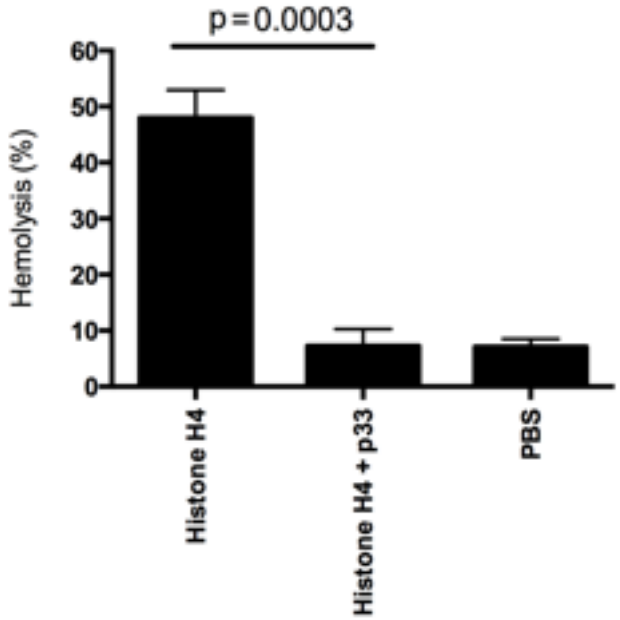
p = 0.0003
Hemolysis (%)
60
50
40
30
20
10
0
Histone H4
Histone H4 + p33
PBS

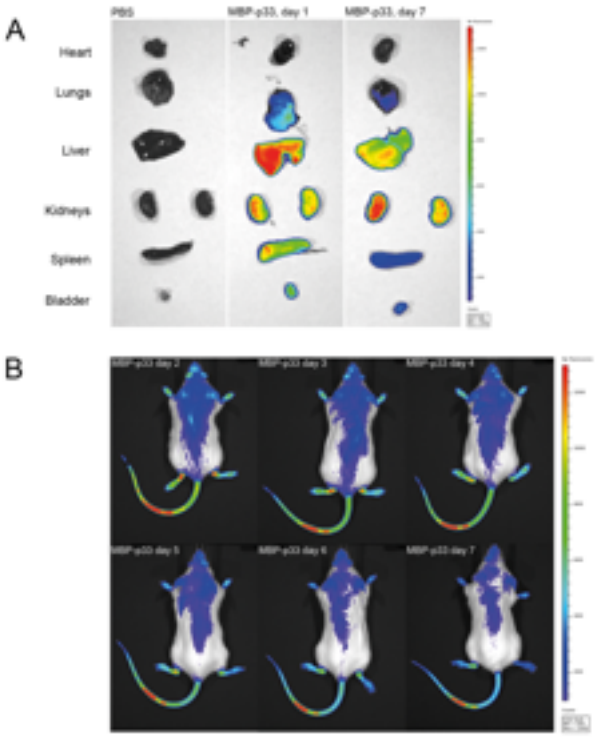
A
PBS
MBP-p33, day 1
MBP-p33, day 7
Heart
Lungs
Liver
Kidneys
Spleen
Bladder
B
MBP-p33 day 2
MBP-p33 day 3
MBP-p33 day 4
MBP-p33 day 5
MBP-p33 day 6
MBP-p33 day 7